AAS 00-168

CASSINI ORBIT DETERMINATION FROM FIRST VENUS FLYBY TO EARTH FLYBY

M.D. Guman, D.C. Roth, R. Ionasescu, T.D. Goodson, A.H. Taylor and J.B. Jones

Navigation and Mission Design Section, Jet Propulsion Laboratory, California Institute of Technology, Pasadena, CA 91109

This paper describes Cassini orbit determination results from the first Venus flyby through the Earth flyby. Emphasis is placed on orbit determination modeling and the resulting orbit solutions. Key solutions supporting maneuver designs are compared against reconstructed trajectory results. Reconstructed maneuver and planetary flyby events are provided.

INTRODUCTION

The Cassini mission is designed to study the planet Saturn and its satellites, rings, and magnetosphere. The Cassini spacecraft, consisting of both a Saturn orbiter and a Titan atmospheric probe, will be injected into orbit around Saturn on 1 July 2004. During the first orbit, the Huygens probe will separate from the orbiter and descend through Titan's atmosphere. The orbiter will continue on a four-year tour of the Saturn system, with multiple close flybys of Titan and several flybys of selected icy satellites.

Cassini's interplanetary trajectory from Earth to Saturn includes gravity assists from two Venus flybys (Venus 1 and Venus 2), an Earth flyby, and a Jupiter flyby. Figure 1 is a diagram of this trajectory as seen from the north ecliptic pole. A previous paper[1] described Cassini orbit determination from launch through the first Venus flyby. The focus of this paper is orbit determination from just past the first Venus flyby through the Earth flyby, the bold portion of the Figure 1 trajectory path.

The Cassini mission was extremely successful during this period, as all orbit determination goals and requirements were met. Orbit determination results were used to achieve several objectives, including maintenance of the actual trajectory to a predefined nominal trajectory, efficient use of propellant, spacecraft safety, mission and science planning, and science data reduction. Most notably, orbit determination performed during this period allowed Cassini to be successfully navigated through flybys of Venus and Earth.

In the following sections, information regarding Cassini orbit determination from the first Venus flyby through the Earth flyby is presented. The spacecraft trajectory is characterized first, followed by a brief description of the impact of Cassini's flight attitude and thruster geometry on the spacecraft's orbital dynamics. Next, orbit determination filter inputs and setup are discussed. These include a description of tracking data and *a priori* models for estimated and considered parameters. Results from selected orbit solutions are presented and compared against the current best reconstructed trajectory.

TRAJECTORY DESCRIPTION

Cassini lift off occurred from Cape Canaveral Air Station aboard a Titan IVB/Centaur launch system at the opening of the launch window on 15 October 1997. Approximately 40 minutes later, the spacecraft was successfully injected into a hyperbolic Earth escape trajectory. An estimate of the spacecraft state at injection was relayed from Lockheed Martin to the Jet Propulsion Laboratory and used as the starting point for the ensuing interplanetary orbit determination analysis.

Five Trajectory Correction Maneuvers (TCMs) were scheduled to occur between the Venus 1 and Venus 2 encounters to ensure Cassini's arrival at the targeted Venus 2 aimpoint on 24 June 1999. TCM4, planned for 14 May 1998 to clean up orbit errors magnified by the Venus 1 flyby, was canceled because it was not needed.[2] The Deep Space Maneuver (DSM) was executed on 3 December 1998 to set up the Venus 2 flyby. The DSM was designed to slow the spacecraft near apoapsis, lowering the subsequent periapsis and increasing the flight path angle at Venus. TCM6 was performed on 4 February 1999 to clean up trajectory errors due mainly to a DSM pointing error. TCM7, executed on 18 May 1999, removed a pre-Venus 2 bias. TCM8, scheduled for 10 June 1999 as a pre-Venus 2 cleanup maneuver, was canceled because it was not needed.[3]

Four maneuvers were performed between the Venus 2 and Earth encounters to target Cassini to its designed Earth flyby aimpoint on 18 August 1999. These maneuvers were executed to incrementally adjust the trajectory to a series of biased aimpoints as set forth in the Cassini Earth Swingby Plan.[4,5] The dates of the maneuvers were as follows: TCM9 on 6 July 1999, TCM10 on 19 July 1999, TCM11 on 2 August 1999 and TCM12 on 11 August 1999. A post-Earth cleanup maneuver, TCM13, was performed on 31 August 1999.

The spacecraft geocentric declination is shown in Figure 2 for the Cassini trajectory between the Venus 1 and Earth flybys. Many previous papers have demonstrated the limitations of Doppler data at low declinations.[6,7] During this period, however, the declination was within 5° of zero for only about 20 days just past the Venus 1 flyby. In the launch to Venus 1 phase of the mission, heliocentric range of the spacecraft was significant because it was nearly constant for portions of the trajectory.[1] This made it difficult to distinguish between the accelerations induced by solar pressure, which vary with the inverse square of heliocentric range, and those induced by the radio-isotope thermoelectric generators (RTGs). For the Venus 1 to Earth phase, however, the heliocentric range varied significantly as shown in Figure 3, allowing for effective separation of these accelerations.

Noteworthy events include aphelion (heliocentric range 1.58 AU) on 7 December 1998, solar opposition on 10 January 1999, perihelion (heliocentric range 0.72 AU) on 29 June 1999 and inferior solar conjunction on 17 August 1999.

FLIGHT ATTITUDE AND CONTROL

The Cassini spacecraft, shown in Figure 4, is three-axis stabilized. While within 2.7 AU of the Sun, the spacecraft -Z axis is nominally pointed at the Sun and the spacecraft -X axis is then pointed as close towards Earth as possible. In this attitude, the high gain antenna (HGA) shades and protects Cassini from adverse thermal conditions while communications are accomplished via one of the two omni-directional low gain antennae (LGA). Exceptions to this orientation exist for limited durations, most notably while executing maneuvers and during a 25 day Instrument Checkout (ICO) period centered around solar opposition on 9 January 1999 (-Z axis is Earth pointed instead of Sun pointed).

During the Venus 1 to Earth period, Cassini's flight attitude was controlled with the Reaction Control Subsystem (RCS), a set of 1 Newton monopropellant thrusters. The RCS is composed of four thruster clusters, each containing four thrusters. Two of the thrusters on each cluster are redundant. Figure 5, a simplified drawing of the plane containing these

thrusters, shows the location and ΔV direction for each thruster. Roll attitude is controlled with the coupled thrusters aligned parallel to the spacecraft Y axis (Y-thrusters). Even though they are coupled, maintaining roll attitude with the Y-thrusters may impart a residual ΔV to the spacecraft because of thruster force mismatch and alignment offsets. These ΔVs have not been observed, however, because they are very small.

Because the Z-thrusters are uncoupled, maintaining pitch and yaw attitude imparts an observable ΔV to the spacecraft in the -Z direction. Since the -Z axis remains Sun pointed, visibility of this ΔV varies with the Earth-spacecraft-Sun angle (Figure 6). The best visibility occurs near solar opposition (Earth-spacecraft-Sun angle = 0°) and solar conjunction (Earth-spacecraft-Sun angle = 180°) when the ΔV is directed along the line of sight. The worst visibility occurs when the angle is around 90° and the ΔV is directed perpendicular to the line of sight.

The RCS is also used to execute small trajectory correction maneuvers. Cassini's main engine, a redundant 445 N bipropellant system, is used to execute large maneuvers. For the Venus 1 to Earth period discussed here, only TCM7 was executed using the RCS. All other TCMs, including the post-Earth TCM13 maneuver, were performed using the main engine.

TRACKING DATA

Cassini is equipped with two low gain and one high gain antennae. Because the HGA has been sun-pointed, the two LGA's have been used to transpond tracking data through most of the inner solar system cruise. The HGA was used during solar opposition and will be used again when the spacecraft heliocentric range exceeds 2.7 AU.

Tracking data was acquired by the Deep Space Network (DSN), with complexes in Spain, Australia, and the United States. X-band one-way Doppler, two-way Doppler and range, and three-way Doppler data types were collected. Two-way data, in which the uplink and downlink stations are the same, were the primary data types utilized for determining Cassini's orbit. One-way Doppler, in which the spacecraft generates the signal downlinked to Earth, and three-way data, in which the uplink and downlink stations are different, are more prone to systematic biases and therefore served primarily as sanity checks on the two-way data. Thirty-four meter aperture Beam Waveguide (BWG) and High-Efficiency (HEF) ground antennae acquired two-way tracking data. These antennae plus the 70 m aperture antennae acquired one-way and three-way data.

Doppler data was generally compressed to five minute intervals and was weighted between 0.2 and 1.0 mm/s (based on a one minute count time). Range data was acquired at intervals varying between 5 and 30 minutes, depending on the available signal strength, and was weighted between 5 m and 100 m. Troposphere and ionosphere calibrations were applied to all data.

Radiometric tracking data was scheduled continuously around the Venus and Earth encounters. Early in the Venus 1 to Venus 2 period, tracking was acquired at one pass per week. Starting at Venus 2 minus 90 days, this was increased to 1 pass per 2 days, and then 1 pass per day starting at Venus 2 minus 50 days. Between Venus 2 and Earth, a level of 2 passes per day was maintained. Generally, coverage was balanced between northern and southern hemisphere passes, enabling a better determination of spacecraft declination. Optical navigation data is not scheduled to begin until one year prior to Saturn orbit insertion.[8]

A PRIORI MODELS

Radiometric tracking data were combined with *a priori* models to refine estimates of several spacecraft dynamic parameters. In addition, certain systematic error sources were 'considered', i.e., some parameter errors were accounted for without actually estimating the

parameters themselves. In this section, *a priori* models from the current best-determined orbit are described. The current best-determined orbit is a reconstruction of the Venus 1 to Earth trajectory and is based on data covering the period from 7 days after Venus 1 closest approach to 15 days after the Earth closest approach. *A priori* models of estimated parameters include the spacecraft state, ΔVs, non-gravitational accelerations, and Earth and Venus ephemerides. *A priori* models of considered parameters include tracking station locations and media calibrations.

Spacecraft State

A priori values and uncertainties constraining the spacecraft state were initially based on state and covariance estimates from the preceding data arc solution. After a few weeks of tracking, these constraints were replaced with a diagonal covariance of essentially infinite variance, allowing orbit solutions to converge more quickly. By this time, the information content of the tracking data alone was sufficient to adequately determine the spacecraft state.

ΔVs

TCMs were modeled as finite burns and 47 events were modeled as impulsive ΔV's, as listed in Tables 1 and 2. Several impulsive ΔVs were associated with each TCM sequence. About 30 minutes prior to a TCM, the Attitude and Articulation Control Subsystem (AACS) deadbands were tightened. Then roll and yaw wind turns were performed to orient the spacecraft to the maneuver attitude. Following the maneuver burn, yaw and roll unwind turns were executed to orient the spacecraft back to its nominal attitude. For all main engine TCMs following the DSM, another set of turns, the pointing-bias-fix wind and unwind turns, were implemented to correct for a ~0.9° pointing bias.[3]

While it is advantageous to acquire tracking data throughout the entire TCM sequence in order to separately estimate the burn and turns, this is not always possible; turning to the designed burn attitude may prevent visibility between ground tracking stations and the spacecraft antennae. For the DSM, TCM6, TCM7 and TCM13, sufficient tracking was obtained to allow separate estimates of the burn and turns for each maneuver. For TCM9 through TCM12, sufficient tracking was not acquired for the duration of each sequence. Therefore, for TCM9 through TCM12, nominal values for the pointing-bias-fix turns were modeled, and the roll and yaw turns were combined with the burn for a 'total' ΔV estimate. Nominal TCM values listed in Table 1 account for whether the maneuver was treated as a burn-only or total ΔV. Reconstructed TCM parameters were estimated with infinite *a priori* uncertainties to ensure that the solutions were driven by the data and not *a priori* assumptions.

Table 1
***A PRIORI* TCM MODELS**

	Start Time (UTC)	*A Priori* Values (Magnitude, RA, DEC) (m/s, deg, deg)
*DSM	03 DEC 1998 06:00:00	(449.962, 3.889, -2.769)
*TCM6	04 FEB 1999 20:00:00	(11.530, 305.054, -10.764)
*TCM7	18 MAY 1999 17:00:00	(0.230, 255.415, -8.534)
†TCM9	06 JUL 1999 17:00:00	(43.544, 265.270, 44.055)
†TCM10	19 JUL 1999 16:00:00	(5.133, 274.781, 66.114)
†TCM11	02 AUG 1999 21:30:00	(36.309, 62.317, 15.339)
†TCM12	11 AUG 1999 15:30:00	(12.256, 293.272, 76.462)
*TCM13	31 AUG 1999 16:00:00	(6.696, 76.304, 24.233)

Note: Right ascension and declination are in Earth Mean Equator of 2000 coordinates.
* TCM modeled as a burn-only ΔV.

† TCM modeled as a total ΔV (burn + roll turns + yaw turns).

Besides the turns associated with TCMs, impulsive ΔVs were modeled to account for other events. One such event was the Probe AGC Exercise occurring on 28 May 1998, which imparted a ΔV of about 10 mm/s to the spacecraft. Reaction Wheel Assembly (RWA) Maintenance Activities, required periodically to lubricate the reaction wheel bearings, caused the RCS to respond with a ΔV of about 1 mm/s as the reaction wheels were spun up. Several events during the ICO period were modeled, including increased RCS thruster firing associated with a spacecraft safing incident. ΔVs associated with RCS firing to counter gravity gradient effects during the Venus 2 and Earth flybys were accounted for. Other activities modeled near the Earth flyby were the VIMS cover release, the Magnetometer Boom (Mag Boom) deployment, and pre- and post-Earth roll turns. Two small ΔVs associated with increased RCS thrusting observed in spacecraft telemetry were modeled after TCM6 and Earth closest approach. These were most likely caused by AACS stabilization, which may occur after TCMs and other significant events. While this phenomenon is usually best modeled with an acceleration (described in the following section), telemetry data occasionally reveals a sudden jump in thruster activity which are more effectively modeled as impulsive ΔVs.

Table 2
***A PRIORI* IMPULSIVE ΔV MODELS**

	Time (UTC)	*A Priori* Value (mm/s)	1-σ *A Priori* Uncertainty (mm/s)
Probe AGC Exercise	28 MAY 1998 21:35:57	(1.0, 0.0, -10.0)	(5.0, 1.0, 5.0)
RWA Maintenance	29 JUN 1998 07:18:57	-1.4	1.0
RWA Maintenance	23 SEP 1998 13:03:57	-1.0	1.0
Pre-DSM AACS Deadband Tightening	03 DEC 1998 05:21:36	0.0	5.0
*DSM Roll Wind Turn	03 DEC 1998 05:37:16	(0.0, 0.0, 0.0)	(1.0, 1.0, 1.0)
*DSM Yaw Wind Turn	03 DEC 1998 05:51:41	(6.1, -4.6, -3.4)	(1.0, 1.0, 1.0)
*DSM Yaw Unwind Turn	03 DEC 1998 07:37:02	(6.1, -4.6, -3.4)	(1.0, 1.0, 1.0)
*DSM Roll Unwind Turn	03 DEC 1998 07:51:27	(0.0, 0.0, 0.0)	(1.0, 1.0, 1.0)
RWA Maintenance	18 DEC 1998 12:28:57	-1.2	1.0
Turn to HGA Earth-Point (ICO)	28 DEC 1998 04:18:57	(-0.5, 0.0, -4.5)	(0.5, 0.5, 2.5)
CAPS/MIMI Activity (ICO)	08 JAN 1999 02:18:26	(-3.1, 0.0, -52.8)	(30.0, 30.0, 30.0)
Spacecraft Safing (ICO)	12 JAN 1999 00:03:56	(0.0, 0.0, 0.0)	(1.0, 1.0, 10.0)
Turn to HGA Earth-Point (ICO)	15 JAN 1999 11:44:56	(-0.5, 0.0, -4.5)	(0.5, 0.5, 2.5)
SPICA Imaging Activity (ICO)	16 JAN 1999 23:34:56	(-3.7, -0.1, -32.1)	(30.0, 30.0, 30.0)
Radar Activity AACS Deadband Tightening (ICO)	18 JAN 1999 21:08:56	0.0	5.0
Turn to HGA Sun-Point (ICO)	21 JAN 1999 19:43:56	(-0.5, 0.0, -4.5)	(0.5, 0.5, 2.5)
Pre-TCM6 AACS Deadband Tightening	04 FEB 1999 19:36:57	0.0	0.5
TCM6 Roll Wind Turn	04 FEB 1999 19:47:34	0.0	1.0
*TCM6 Yaw Wind Turn	04 FEB 1999 19:54:19	(6.1, -8.1, -3.5)	(1.0, 1.0, 1.0)
*TCM6 Pointing-Bias-Fix Wind Turn	04 FEB 1999 19:55:52	(2.4, -2.8, -1.0)	(1.0, 1.0, 1.0)
*TCM6 Pointing-Bias-Fix Unwind Turn	04 FEB 1999 20:02:41	(2.4, -2.8, -1.0)	(1.0, 1.0, 1.0)
*TCM6 Yaw Unwind Turn	04 FEB 1999 20:05:15	(6.1, -8.1, -3.5)	(1.0, 1.0, 1.0)
TCM6 Roll Unwind Turn	04 FEB 1999 20:12:00	0.0	1.0
Post-TCM6 AACS Stabilization	04 FEB 1999 22:58:56	0.0	0.5
RWA Maintenance	09 MAR 1999 15:58:56	-1.0	0.5
*TCM7 Yaw Wind Turn	18 MAY 1999 16:50:52	(5.0, -5.4, -1.1)	(1.0, 1.0, 1.0)
*TCM7 Yaw Unwind Turn	18 MAY 1999 17:12:24	(5.0, -5.4, -1.1)	(1.0, 1.0, 1.0)
RWA Maintenance	19 JUN 1999 20:23:56	-1.2	0.5
RCS Firing to Counter Venus Gravity Gradient	24 JUN 1999 20:29:55	-0.7	0.5
Pre-TCM9 AACS Deadband Tightening	06 JUL 1999 16:26:16	-3.0	1.0
Pre-TCM10 AACS Deadband Tightening	19 JUL 1999 15:27:31	-3.0	1.0
Pre-TCM11 AACS Deadband Tightening	02 AUG 1999 20:53:28	-3.0	1.0
Pre-TCM12 AACS Deadband Tightening	11 AUG 1999 14:57:50	-3.0	1.0

VIMS Cover Release	15 AUG 1999 20:42:00	0.0	1.0
Magnetometer Boom Deployment	16 AUG 1999 06:53:21	-2.0	1.0
Pre-Earth Roll Turn	17 AUG 1999 21:28:21	0.0	1.0
Pre-Earth AACS Deadband Tightening	17 AUG 1999 22:12:48	-3.0	1.0
RCS Firing to Counter Earth Gravity Gradient	18 AUG 1999 03:31:12	-0.6	1.0
Post-Earth Roll Turn	18 AUG 1999 06:13:00	0.0	1.0
Post-Earth AACS Stabilization	18 AUG 1999 09:18:00	0.0	1.0
Pre-TCM13 AACS Deadband Tightening	31 AUG 1999 15:33:05	-3.0	1.0
TCM13 Roll Wind Turn	31 AUG 1999 15:43:09	0.0	1.0
*TCM13 Yaw Wind Turn	31 AUG 1999 15:51:47	(-4.7, 7.3, 4.3)	(1.0, 1.0, 1.0)
*TCM13 Pointing-Bias-Fix Wind Turn	31 AUG 1999 15:55:47	(0.8, 3.4, 1.6)	(1.0, 1.0, 1.0)
*TCM13 Pointing-Bias-Fix Unwind Turn	31 AUG 1999 16:01:48	(0.8, 3.4, 1.6)	(1.0, 1.0, 1.0)
*TCM13 Yaw Unwind Turn	31 AUG 1999 16:06:48	(-4.7, 7.3, 4.3)	(1.0, 1.0, 1.0)
TCM13 Roll Unwind Turn	31 AUG 1999 16:15:32	0.0	1.0

Note: Asterisk (*) indicates ΔV in Earth Mean Equator of 2000 coordinates, otherwise in spacecraft-fixed coordinates. Single values indicate only spacecraft-fixed z-component estimated.

Non-gravitational Accelerations

Two accelerations spanning the entire data arc and several others spanning only a few days were estimated, as listed in Table 3. Accelerations induced by solar pressure and asymmetric radio-isotope thermoelectric generator (RTG) radiation forces span the entire data arc. Short duration accelerations have also been observed after several of the events listed in Tables 1 and 2.

Table 3
***A PRIORI* NON-GRAVITATIONAL ACCELERATION MODELS**

	Time Span (UTC)	***A Priori* Values**
Solar Pressure (m^2)	Pre- Mag Boom deployment	(0.00, 0.04, 20.92)
Solar Torque (m^3)	Pre- Mag Boom deployment	(3.55, -1.05, 0.00)
RTG Radiation (km/s^2)	Entire Arc	$(-0.9, -0.1, -7.5) \times 10^{-12}$
Post-TCM7 Accel. (km/s^2) and *Time Constant (hours)	18 MAY 1999 18:00 to 19 MAY 1999 04:30	0.0 5.0
Post-TCM9 Accel. (km/s^2) and Time Constant (hours)	06 JUL 1999 17:30 to 08 JUL 1999 09:30	-18.0×10^{-12} 7.0
Post-TCM10 Accel. (km/s^2) and Time Constant (hours)	19 JUL 1999 16:22 to 20 JUL 1999 21:22	-18.0×10^{-12} 7.0
Post-TCM11 Accel. (km/s^2) and Time Constant (hours)	02 AUG 1999 22:02 to 03 AUG 1999 12:02	-18.0×10^{-12} 7.0
Post-TCM12 Accel. (km/s^2) and Time Constant (hours)	11 AUG 1999 15:53 to 13 AUG 1999 02:53	-18.0×10^{-12} 7.0
Post-Mag Boom Deployment Accel. (km/s^2) and Time Constant (hours)	16 AUG 1999 06:54 to 17 AUG 1999 21:25	-1.0×10^{-12} 7.0
Post-TCM13 Accel. (km/s^2) and Time Constant (hours)	31 AUG 1999 16:17 to 02 SEP 1999 02:00	-18.0×10^{-12} 7.0

Note: Spacecraft-fixed coordinates. Single acceleration values indicate only spacecraft-fixed z-component estimated.
* Time constant modeled but not estimated for this acceleration.

The largest of the estimated accelerations is due to solar pressure. Solar pressure induced accelerations vary with the inverse square of heliocentric range and may be separated into two parts. First, there is a direct effect accelerating the spacecraft away from the sun. Second, there is an indirect effect caused by the RCS' response to spacecraft torques induced by solar pressure. Z-thrusters fire to counter torques and, because the spacecraft is Sun-pointed, will accelerate the spacecraft towards the sun. Prior to the Mag

Boom deployment, the direct effect was around seven times larger than the indirect effect. At perihelion, just after the Venus 2 flyby, the direct nominal acceleration was 32 x 10^{-12} km/s^2. After the Mag Boom deployment, direct and indirect solar pressure effects were predicted to be nearly the same magnitude - the two effects would nearly cancel each other. Because of the Mag Boom's long moment arm, the direct solar pressure effect increased by around 18%, while the indirect effect increased by more than 700%.

An *a priori* uncertainty of approximately 3.5% of the nominal value constrains the estimates of the solar pressure direct accelerations. Solar pressure effective areas, a synthesis of the actual sunlit areas and reflectivity coefficients, were estimated for the direct effect. An *a priori* uncertainty of 100% of the nominal value constrains the estimates of the solar torque accelerations. The combination of solar pressure effective areas times an effective moment arm were estimated for the indirect effect. The large proportional *a priori* uncertainty was used for the solar torque model to account for such inefficiencies as RCS double-sided limit cycling. Estimates of solar pressure and solar torque parameters after the Mag Boom deployment are not included here because the tracking data arc is very short and subject to many z-thruster events which tend to corrupt the estimate. The nominal post-Mag Boom solar torque value of (27.07, -1.23, 0.00) m^3 is expected to be the best estimate.

Another acceleration spanning the entire data arc is due to asymmetric radiation forces from the spacecraft RTGs. Three RTGs are located in a plane perpendicular to the z-axis near the base of the spacecraft. Radiation from these sources is emitted in all directions but is partially reflected back by the high gain antenna and shielding. This reflectance has the effect of accelerating the spacecraft in the -z direction, or towards the Sun. Because the RTG power degrades with a time constant of over 100 years, this force is constant for all practical purposes and is modeled as such. *A priori* 1-σ uncertainties in the RTG acceleration components were assumed to be 50% of their nominal values, as derived from Reference 9.

Several short duration accelerations have also been estimated. These acceleration models extend for at most a few days and are caused by z-thruster firings above the level required to control spacecraft torques induced by solar pressure and the RTGs. Short-term accelerations associated with post-maneuver RCS thrusting for TCM7 through TCM13 have been modeled, as well as one that accounts for thrusting observed after the Mag Boom deployment. All short duration accelerations were modeled as decaying exponential functions, defined by initial acceleration values and time constants. Infinite *a priori* uncertainties were used in the estimation of these parameters. Thruster telemetry has been useful in constructing model inputs for these events. Activity in the Z3 thruster was closely correlated to the occurrence of RCS double-sided limit cycling and was therefore a reliable indicator of thrusting above nominal levels. Figure 7 shows Z3 thruster cumulative on-time telemetry data plotted for the period immediately following TCM12. The thrusting profile, approximately exponential in nature, is clearly seen in the telemetry. Start and end times for the acceleration were easily extracted from the data and implemented to the model. In addition, estimated accelerations and time constants were compared to the telemetry for corroboration. This procedure was used to effectively characterize and model each of the short duration accelerations from Venus 1 to Earth.

Other *A Priori* Models

To adequately fit the tracking data acquired during the Venus and Earth flybys, Earth and Venus ephemerides were estimated. *A priori* ephemeris values and uncertainties are from planetary ephemeris DE-405. Tracking station locations and media calibrations were considered, i.e., accounted for without being estimated. Station locations are from Reference 10, except Deep Space Stations (DSS) 34 and 54, which have since been modified to include the results of recent surveys. *A priori* station location uncertainties of 0.5 m are modeled. Media calibrations are provided by the Tracking System and Analytic Calibration group at JPL. *A priori* uncertainties for dry and wet troposphere calibrations are 1 and 4 cm

respectively. *A priori* uncertainties for night and day ionosphere calibrations are 1 and 5 cm respectively.

ORBIT DETERMINATION RESULTS

Many orbit determination solutions were generated and analyzed from the Venus 1 flyby through the Earth flyby. Sensitivities to various combinations of data types, data weights, data arc lengths, *a priori* values and uncertainties, and other factors were analyzed. Orbit determination results discussed in this section represent key solutions used to design TCMs and reconstruct the Venus 1 to Earth trajectory. Table 4 lists the names, purposes, and tracking data arc lengths of these orbit determination solutions. The naming convention refers to when orbit determination products became available. For instance, V2M48D specifies product availability at **V**enus **2** **M**inus **48** **D**ays, EM22D at **E**arth **M**inus **22** **D**ays.

Table 4
SUMMARY OF SELECTED ORBIT SOLUTIONS

Identifier	Purpose	Data Arc Start (UTC)	Data Arc End (UTC)
V2M189D	DSM reconstruction	03 MAY 1998	14 DEC 1998
V2M148D	TCM6 final design	03 MAY 1998	27 JAN 1999
V2M113D	TCM6 reconstruction	22 JAN 1999	25 FEB 1999
V2M48D	TCM7 final design	05 FEB 1999	07 MAY 1999
EM52D	TCM9 final design	05 FEB 1999	27 JUN 1999
EM49D	TCM7 reconstruction	05 FEB 1999	30 JUN 1999
EM36D	TCM10 final design	26 JUN 1999	13 JUL 1999
EM28D	TCM9 reconstruction	26 JUN 1999	19 JUL 1999
EM22D	TCM11 final design	26 JUN 1999	27 JUL 1999
EM15D	TCM10 reconstruction	26 JUN 1999	02 AUG 1999
EM11D	TCM12 final design	26 JUN 1999	07 AUG 1999
EM5D	TCM11 reconstruction	26 JUN 1999	11 AUG 1999
EM1D	TCM12 reconstruction	26 JUN 1999	17 AUG 1999
EP6D	TCM13 final design	26 JUN 1999	24 AUG 1999
EP50D	TCM13 reconstruction	19 AUG 1999	11 SEP 1999
Venus 2 Reconstruction	Venus 2 flyby reconstruction	03 MAY 1998	06 JUL 1999
Earth Reconstruction	Earth flyby reconstruction	26 JUN 1999	02 SEP 1999

The solutions presented in this section provide a history of the best orbit determination knowledge available at selected times. In addition, orbit determination performance is reviewed by removing the effects of maneuver execution errors from orbit estimates, mapping solutions to either the Venus 2 or Earth B-plane at closest approach, and then comparing the results. Finally, parameter estimates from the trajectory reconstruction are tabulated and discussed.

TCM Reconstruction

Trajectory correction maneuvers are routinely reconstructed in an effort to determine and calibrate thruster performance. All TCMs in the Venus 1 to Earth period, including TCM13 just past the Earth flyby, have been reconstructed. Estimates for these maneuvers, along with formal *a posteriori* uncertainties, are listed in Table 5. As described previously, some of the TCMs were estimated as burn-only ΔVs, while others were treated as total ΔVs (burn plus yaw turns and roll turns), depending on the availability of tracking data through the maneuver sequence.

Comparing the estimated TCM values to the nominal values presented in Table 1, magnitude errors were small for all of the TCMs and well within maneuver execution error requirements.[8] The DSM had a slight overburn, with all of the other TCMs exhibiting slight underburns. Pointing requirements were also met, although the DSM was characterized by a ~0.9° pointing error. This error was determined to be caused by a bias in main engine pointing.[3] As a result, all subsequent main engine maneuver sequences included a set of pointing-bias-fix turns to remove the offset.

Table 5
TCM ESTIMATES

	Estimated Values (Magnitude, RA, DEC) (m/s, deg, deg)	1-σ *A Posteriori* Uncertainty (Magnitude, RA, DEC) (m/s, deg, deg)
*DSM	(450.219, 4.832, -2.773)	(0.003, < 0.001, < 0.001)
*TCM6	(11.519, 305.092, -10.696)	(0.007, 0.042, 0.135)
*TCM7	(0.225, 256.213, -9.619)	(< 0.001, 0.232, 0.494)
†TCM9	(43.485, 265.125, 44.006)	(0.015, 0.002, 0.009)
†TCM10	(5.130, 274.509, 66.091)	(0.006, 0.016, 0.009)
†TCM11	(36.288, 62.273, 15.436)	(0.003, 0.003, 0.010)
†TCM12	(12.246, 292.877, 76.473)	(0.003, 0.021, 0.004)
*TCM13	(6.685, 76.336, 24.544)	(0.008, 0.014, 0.118)

Note: Right ascension and declination are in Earth Mean Equator of 2000 coordinates.
* TCM modeled as a burn-only ΔV.
† TCM modeled as a total ΔV (burn + roll turns + yaw turns).

TCM Design Support

One of the primary uses of orbit determination results is for correcting a spacecraft's orbit to the predefined nominal trajectory. For Cassini, the period discussed here is significant because its nominal trajectory included flybys of the planets Venus and Earth. Orbit determination solutions were generated to support preliminary and final designs for all of the TCMs in the Venus 1 to Earth period. The final TCM design solutions and the uncertainties associated with them have been mapped to the Venus 2 and Earth B-planes at closest approach (the Appendix contains a description of the B-plane coordinate system) and are presented as a series of plots in Figure 8 (Venus 2 approach) and Figure 9 (Earth approach). For reference, TCM and flyby aimpoints and surface impact radii for Venus and Earth are also plotted. In Figure 8a, the offset between the V2M148D solution (TCM6 design) and the DSM/TCM6 aimpoint represents trajectory error due mainly to the ~0.9° pointing bias in the DSM maneuver. Figure 8b zooms in on an area closer to Venus, where the V2M48D (TCM7 design) solution is depicted relative to the TCM6 and TCM7 aimpoints. Figure 8c shows Cassini's closest approach to Venus based on the reconstructed trajectory, and Figure 8d zooms in on the 1-σ uncertainty ellipse of the reconstructed flyby point. The dimensions of the ellipse are approximately 100 m by 22 m.

Figure 9 is a similar set of plots generated for the approach to Earth. Figure 9a is a B-plane summary of the biased aimpoint approach strategy,[4,5] including aimpoints of TCM9 through TCM12 and Earth's surface impact radius. Figures 9b, 9c, and 9d each zoom-in on an area showing a particular aimpoint and the final orbit determination solution for the upcoming maneuver. Figure 9e shows Cassini's closest approach to Earth based on the reconstructed trajectory, and Figure 9f zooms in on the associated 1-σ error ellipse, with dimensions of about 30 m by 23 m.

Estimated values and uncertainties of the time of closest approach (TCA), a measure of orbit uncertainties perpendicular to the B-plane, are presented in Table 6 for the TCM

final design orbit determination solutions. Changes in the TCA estimates in Table 6 are due to the execution of TCMs and are closely correlated with changes in B•T. Therefore, large changes in B•T, such as between the V2M148D and V2M48D solutions, account for the largest changes in TCA. Similarly, the B•T values are close for the EM36D and EM22D solutions, resulting in similar TCA estimates. The uncertainties in TCA can be approximately converted to downtrack position uncertainties by multiplying by the V_∞ of the appropriate flyby (9.4 km/s for Venus 2 and 16.0 km/s for Earth). This calculation results in about 50 m of downtrack uncertainty in both the Venus 2 and Earth reconstructed flybys.

Table 6
TIME OF CLOSEST APPROACH FOR SELECTED ORBIT SOLUTIONS

	TCA Relative To:	Time of Closest Approach (UTC)	1-σ *A Posteriori* Uncertainty (sec)
V2M148D	Venus 2	25 JUN 1999 02:40:43.341	66.180
V2M48D	Venus 2	24 JUN 1999 20:29:16.309	1.195
Venus 2 Reconstruction	Venus 2	24 JUN 1999 20:29:54.892	0.005
EM52D	Earth	18 AUG 1999 04:03:20.838	0.688
EM36D	Earth	18 AUG 1999 03:29:06.284	0.082
EM22D	Earth	18 AUG 1999 03:29:04.111	0.047
EM11D	Earth	18 AUG 1999 03:28:36.467	0.107
Earth Reconstruction	Earth	18 AUG 1999 03:28:25.614	0.003

Orbit Determination Performance

While Figures 8 and 9 are useful for depicting where various orbit solutions are positioned relative to aimpoints, they do not provide a direct means of evaluating orbit determination performance. That is, differences between trajectory estimates and designed aimpoints shown in Figures 8 and 9 include the effects of maneuver execution errors and unanticipated downstream ΔVs acting on the spacecraft (such as anomalous RCS firings or a safing event), to go along with possible orbit determination errors. To evaluate orbit determination performance, the error ellipses from Figures 8 and 9 are repeated in Figures 10 and 11, with the difference that the shifts in orbit solutions attributable to TCMs, other ΔVs and short duration accelerations have been eliminated. That is, all disturbances downstream of the data cutoff time for a particular solution are modeled with values from the *reconstructed* solution, taken to be the truth model. Solutions are plotted relative to the trajectory reconstruction solution instead of the center of Venus or Earth. Figure 10a shows that the TCM6 and TCM7 design solutions (V2M148D and V2M48D, respectively) are consistent (within 1-σ) with each other and the reconstructed solution (represented by the 'x' at the origin). The larger ellipse associated with the V2M148D solution arises from uncertainties in estimating ICO activities prior to TCM6. Figure 10b focuses in on the V2M48D solution.

Figure 11 shows that for three out of the four Earth approach solutions, the reconstructed trajectory lies within the delivered 1-σ uncertainty ellipse. The TCM10 design solution (EM36D) is about 2-σ from the reconstructed trajectory. Additional analysis revealed that most of the EM36D solution offset was caused by an increased sensitivity to media calibrations.

Reconstruction of Venus 2 and Earth Flybys

Flyby trajectories can be reconstructed very accurately when tracking data is acquired on both the incoming and outgoing trajectory asymptotes. This was the case for both the Venus 2 and Earth flyby reconstructions. The reconstructed flyby point for Venus 2 was estimated to be 3,307.297 ± 0.074 km B•R, -9,064.874 ± 0.071 km B•T, and a time of

closest approach of 24 June 1999 20:29:54.892 ± 0.005 UTC. This corresponds to a difference of only 11 km in the B-plane and 2.5 s in TCA when compared to the designed flyby aimpoint. The reconstructed flyby point for Earth was estimated to be 167.065 ± 0.030 km B•R, 8968.915 ± 0.023 km B•T, and a time of closest approach of 18 AUG 1999 03:28:25.614 ± 0.003 UTC. This corresponds to a difference of only 9 km in the B-plane and less than 1 s in TCA when compared to the designed flyby aimpoint. Two-way Doppler and range residual plots for the reconstructed trajectories are included in Figures 12 and 13.

Table 7
IMPULSIVE ΔV ESTIMATES

	Time (UTC)	Estimated Value (mm/s)	1-σ *A Posteriori* Uncertainty (mm/s)
Probe AGC Exercise	28 MAY 1998 21:35:57	(1.3, -0.2, -10.4)	(0.1, 1.1, 0.1)
RWA Maintenance	29 JUN 1998 07:18:57	-1.5	< 0.1
RWA Maintenance	23 SEP 1998 13:03:57	-1.3	< 0.1
Pre-DSM AACS Deadband Tightening	03 DEC 1998 05:21:36	-1.7	0.1
*DSM Roll Wind Turn	03 DEC 1998 05:37:16	(0.5, -0.7, -0.3)	(0.8, 0.7, 0.9)
*DSM Yaw Wind Turn	03 DEC 1998 05:51:41	(6.5, -5.2, -3.7)	(0.8, 0.7, 0.9)
*DSM Yaw Unwind Turn	03 DEC 1998 07:37:02	(7.2, -6.0, -4.1)	(0.8, 0.7, 0.9)
*DSM Roll Unwind Turn	03 DEC 1998 07:51:27	(0.4, -0.5, -0.3)	(0.8, 0.7, 0.9)
RWA Maintenance	18 DEC 1998 12:28:57	-1.3	< 0.1
Turn to HGA Earth-Point (ICO)	28 DEC 1998 04:18:57	(-0.4, 0.1, -9.9)	(0.5, 0.5, 0.1)
CAPS/MIMI Activity (ICO)	08 JAN 1999 02:18:26	(-40.4, -18.2, -73.3)	(10.6, 8.9, 0.4)
Spacecraft Safing (ICO)	12 JAN 1999 00:03:56	(0.0, 0.0, -7.1)	(1.0, 1.0, 0.3)
Turn to HGA Earth-Point (ICO)	15 JAN 1999 11:44:56	(-0.6, 0.0, -6.3)	(0.5, 0.5, 0.3)
SPICA Imaging Activity (ICO)	16 JAN 1999 23:34:56	(12.2, -53.2, -56.3)	(7.7, 12.7, 0.4)
Radar Activity AACS Deadband Tightening (ICO)	18 JAN 1999 21:08:56	-3.4	0.3
Turn to HGA Sun-Point (ICO)	21 JAN 1999 19:43:56	(-0.5, 0.0, -7.1)	(0.5, 0.5, 0.1)
Pre-TCM6 AACS Deadband Tightening	04 FEB 1999 19:36:57	-2.9	0.6
TCM6 Roll Wind Turn	04 FEB 1999 19:47:34	-0.3	0.6
*TCM6 Yaw Wind Turn	04 FEB 1999 19:54:19	(6.2, -8.3, -3.6)	(1.0, 0.8, 0.9)
*TCM6 Pointing-Bias-Fix Wind Turn	04 FEB 1999 19:55:52	(2.4, -2.9, -1.1)	(1.0, 0.8, 0.9)
*TCM6 Pointing-Bias-Fix Unwind Turn	04 FEB 1999 20:02:41	(2.4, -2.9, -1.1)	(1.0, 0.9, 1.0)
*TCM6 Yaw Unwind Turn	04 FEB 1999 20:05:15	(6.2, -8.3, -3.6)	(1.0, 0.8, 0.9)
TCM6 Roll Unwind Turn	04 FEB 1999 20:12:00	-0.4	0.4
Post-TCM6 AACS Stabilization	04 FEB 1999 22:58:56	-0.4	0.1
RWA Maintenance	09 MAR 1999 15:58:56	-1.6	< 0.1
*TCM7 Yaw Wind Turn	18 MAY 1999 16:50:52	(5.3, -5.9, -1.3)	(0.8, 0.8, 1.0)
*TCM7 Yaw Unwind Turn	18 MAY 1999 17:12:24	(5.5, -6.2, -1.5)	(0.8, 0.8, 1.0)
RWA Maintenance	19 JUN 1999 20:23:56	-1.3	0.3
RCS Firing to Counter Venus Gravity Gradient	24 JUN 1999 20:29:55	-0.7	0.4
Pre-TCM9 AACS Deadband Tightening	06 JUL 1999 16:26:16	-2.8	0.2
Pre-TCM10 AACS Deadband Tightening	19 JUL 1999 15:27:31	-3.2	0.1
Pre-TCM11 AACS Deadband Tightening	02 AUG 1999 20:53:28	-2.7	0.1
Pre-TCM12 AACS Deadband Tightening	11 AUG 1999 14:57:50	-2.3	0.1
VIMS Cover Release	15 AUG 1999 20:42:00	-0.1	< 0.1
Magnetometer Boom Deployment	16 AUG 1999 06:53:21	-1.9	0.1
Pre-Earth Roll Turn	17 AUG 1999 21:28:21	-0.6	0.1
Pre-Earth AACS Deadband Tightening	17 AUG 1999 22:12:48	-2.9	0.1
RCS Firing to Counter Earth Gravity Gradient	18 AUG 1999 03:31:12	-1.9	0.1
Post-Earth Roll Turn	18 AUG 1999 06:13:00	0.2	0.2
Post-Earth AACS Stabilization	18 AUG 1999 09:18:00	-0.2	< 0.1
Pre-TCM13 AACS Deadband Tightening	31 AUG 1999 15:33:05	-2.9	0.1
TCM13 Roll Wind Turn	31 AUG 1999 15:43:09	-0.6	0.1
*TCM13 Yaw Wind Turn	31 AUG 1999 15:51:47	(-5.1, 7.4, 4.3)	(0.4, 1.0, 1.0)
*TCM13 Pointing-Bias-Fix Wind Turn	31 AUG 1999 15:55:47	(0.8, 3.4, 1.6)	(0.4, 1.0, 1.0)
*TCM13 Pointing-Bias-Fix Unwind Turn	31 AUG 1999 16:01:48	(1.2, 3.3, 1.5)	(0.5, 1.0, 1.0)
*TCM13 Yaw Unwind Turn	31 AUG 1999 16:06:48	(-5.2, 7.4, 4.3)	(0.3, 1.0, 1.0)
TCM13 Roll Unwind Turn	31 AUG 1999 16:15:32	0.1	0.2

Note: Asterisk (*) indicates ΔV in Earth Mean Equator of 2000 coordinates, otherwise in spacecraft-fixed coordinates. Single values indicate only spacecraft-fixed z-component estimated.

Table 8
NON-GRAVITATIONAL ACCELERATION ESTIMATES

	Estimated Values	1-σ *A Posteriori* Uncertainty
Solar Pressure (m^2)	(-0.08, -0.12, 21.10)	(0.04, 0.12, 0.65)
Solar Torque (m^3)	(3.87, -1.14, 0.00)	(0.81, 0.26, < 0.01)
RTG Radiation (km/s^2)	(-1.1, -0.1, -2.7) x 10^{-12}	(0.4, 0.1, 0.6) x 10^{-12}
Post-TCM7 Accel. (km/s^2) and *Time Constant (hours)	-1.9 x 10^{-12} -	2.4 x 10^{-12} -
Post-TCM9 Accel. (km/s^2) and Time Constant (hours)	-21.6 x 10^{-12} 5.1	13.7 x 10^{-12} 1.9
Post-TCM10 Accel. (km/s^2) and Time Constant (hours)	-16.2 x 10^{-12} 7.2	6.6 x 10^{-12} 2.0
Post-TCM11 Accel. (km/s^2) and Time Constant (hours)	-9.7 x 10^{-12} 5.2	8.4 x 10^{-12} 3.7
Post-TCM12 Accel. (km/s^2) and Time Constant (hours)	-14.2 x 10^{-12} 7.9	4.4 x 10^{-12} 1.8
Post-Mag Boom Deployment Accel. (km/s^2) and Time Constant (hours)	-2.0 x 10^{-12} 27.5	1.8 x 10^{-12} 36.5
Post-TCM13 Accel. (km/s^2) and Time Constant (hours)	-6.4 x 10^{-12} 11.2	2.7 x 10^{-12} 5.7

Note: Spacecraft-fixed coordinates. Single acceleration values indicate only spacecraft-fixed z-component estimated.
* Time constant modeled as 5 hours but not estimated for this acceleration.

Estimated parameters and formal one sigma *a posteriori* uncertainties are listed in Tables 7 and 8. Several values deserve some attention. ΔV events with repeated occurrences were quite consistent in the Venus 1 to Earth period. One set of these, the five RWA maintenance activity ΔVs, were all estimated to within 0.2 mm/s of –1.2 mm/s. Another group of ΔVs, the nine AACS deadband tightenings, had a mean of –2.8 mm/s with a standard deviation of 0.5 mm/s. This consistency allowed the pre-maneuver AACS deadband tightenings to be modeled in TCM design solutions (starting with TCM9) in an effort to reduce ΔV errors.

Estimates of post-maneuver accelerations for the four main engine pre-Earth TCMs varied from –9.7 x 10^{-12} km/s^2 to –21.6 x 10^{-12} km/s^2. Associated time constants ranged from 5.1 to 7.9 days. There does not seem to be a correlation between the size of the maneuver and the size of the post-maneuver acceleration. If further analysis could determine the dependence of post-maneuver accelerations, they could be modeled in future TCM designs, further reducing maneuver ΔV errors.

In a previous paper covering orbit determination results for the launch to Venus 1 period,[1] several inconsistencies in estimated long-term accelerations suggested some mismodeling of those parameters. In particular, the z-component of the solar pressure model represented a four sigma change from the nominal value of 20.9 m^2, and the z-component of the RTG radiation model was positive when it should have been negative. These inconsistencies are not present in the Venus 1 to Earth results presented here. Specifically, the estimated z-component of the solar pressure model is within one sigma of the nominal value, and the the z-component of the RTG radiation model has the proper polarity. One reason for this is the inclusion of solar torque modeling here which was not included in the launch to Venus 1 modeling. Also, more variation in the heliocentric range during the Venus 1 to Earth period allowed the RTG acceleration to be distinguished from the solar radiation pressure acceleration.

Venus and Earth planet corrections in radial, downtrack, and out-of-plane coordinates are listed in Table 8. For comparison, the one sigma *a priori* uncertainties for Earth and Venus are (0.01, 2.25, 3.20) km and (0.18, 2.13, 3.38) km, respectively. Only the estimated Venus out-of-plane correction is larger than its a priori uncertainty (by about 1.3 sigma).

Table 8
VENUS AND EARTH EPHEMERIDES CORRECTION ESTIMATES

	Radial (km)	Downtrack (km)	Crosstrack (km)
Earth	< 0.001	0.17	2.35
Venus	-0.14	1.58	4.30

CONCLUDING REMARKS

The Venus 1 to Earth period of the Cassini mission was extremely successful, as all orbit determination goals were met or exceeded. The spacecraft was navigated through the Venus 2 and Earth flybys, both to within about 10 km of the desired B-plane aimpoint for each flyby. Maneuver reconstructions were performed to support maneuver performance analyses, and orbit determination solutions were used in the design of trajectory correction maneuvers. Modeling of post-maneuver accelerations was improved with the use of thruster telemetry data, and repeating ΔV events, such as RWA maintenance activities and attitude control deadband tightenings, were characterized. Experience gained during this phase of the mission will be very important in future phases of the mission as Cassini undertakes new navigation challenges such as the Huygens probe delivery and the tour of Saturn's system.

ACKNOWLEDGEMENTS

The research described in this paper was performed at the Jet Propulsion Laboratory, California Institute of Technology, under contract with the National Aeronautics and Space Administration.

REFERENCES

1. Roth, D.C., M.D. Guman, R. Ionasescu and A.H. Taylor, "Cassini Orbit Determination From Launch to the First Venus Flyby", AIAA/AAS Astrodynamics Specialist Conference, Boston, Massachusetts, 10-12 August 1998.

2. Goodson, T.D., D.L. Gray, Y. Hahn and F. Peralta, "Cassini Maneuver Experience: Launch and Early Cruise", AIAA Guidance, Navigation and Control Conference, Boston, Massachusetts, 10-12 August 1998.

3. Goodson, T.D., D.L. Gray, Y. Hahn and F. Peralta, "Cassini Maneuver Experience: Finishing Inner Cruise", AAS/AIAA Space Flight Mechanics Meeting, Clearwater, Florida, 23-26 January 2000.

4. "Cassini Program Environmental Impact Statement Supporting Study. Volume 3: Cassini Earth Swingby Plan", JPL Internal Document 699-70-3, 18 November 1993.

5. "Cassini Earth Swingby Plan Supplement", JPL Internal Document D-10178-3, May 1997.

6. Hamilton, T.W., and W.G. Melbourne, "Information Content of a Single Pass of Doppler Data From a Distant Spacecraft", JPL Space Programs Summary, No. 37-39, Vol. III, March-April 1966.

7. Thurman, S.W., "Comparison of Earth-Based Radio Metric Data Strategies for Deep Space Navigation", AIAA/AAS Astrodynamics Conference, Portland, Oregon, 20-22 August 1990.

8. "Cassini Navigation Plan", Cassini Project Document 699-101 (JPL Internal Document), 29 May 1996.

9. Lisman, S., "Cassini Non-Gravitational Force and Torque Estimates, Final Guidance Analysis Book Documentation", JPL Interoffice Memorandum 3456-94-004 (JPL Internal Document), 8 August 1994.

10. Folkner, W.M., "Current DSN Station Locations", JPL Interoffice Memorandum 335.1-95-027 (JPL Internal Document), 16 October 1995.

APPENDIX

The B-plane, shown in Figure 12, is a plane passing through the center of the target body and perpendicular to the incoming asymptote of the hyperbolic flyby trajectory. Coordinates in the plane are given in the **R** and **T** directions, with T being parallel to the Earth Mean Orbital plane of 2000. The angle θ determines the rotation of the semi-major axis of the error ellipse in the B-plane relative to the T-axis and is measured positive right-handed about S.

Fig 1

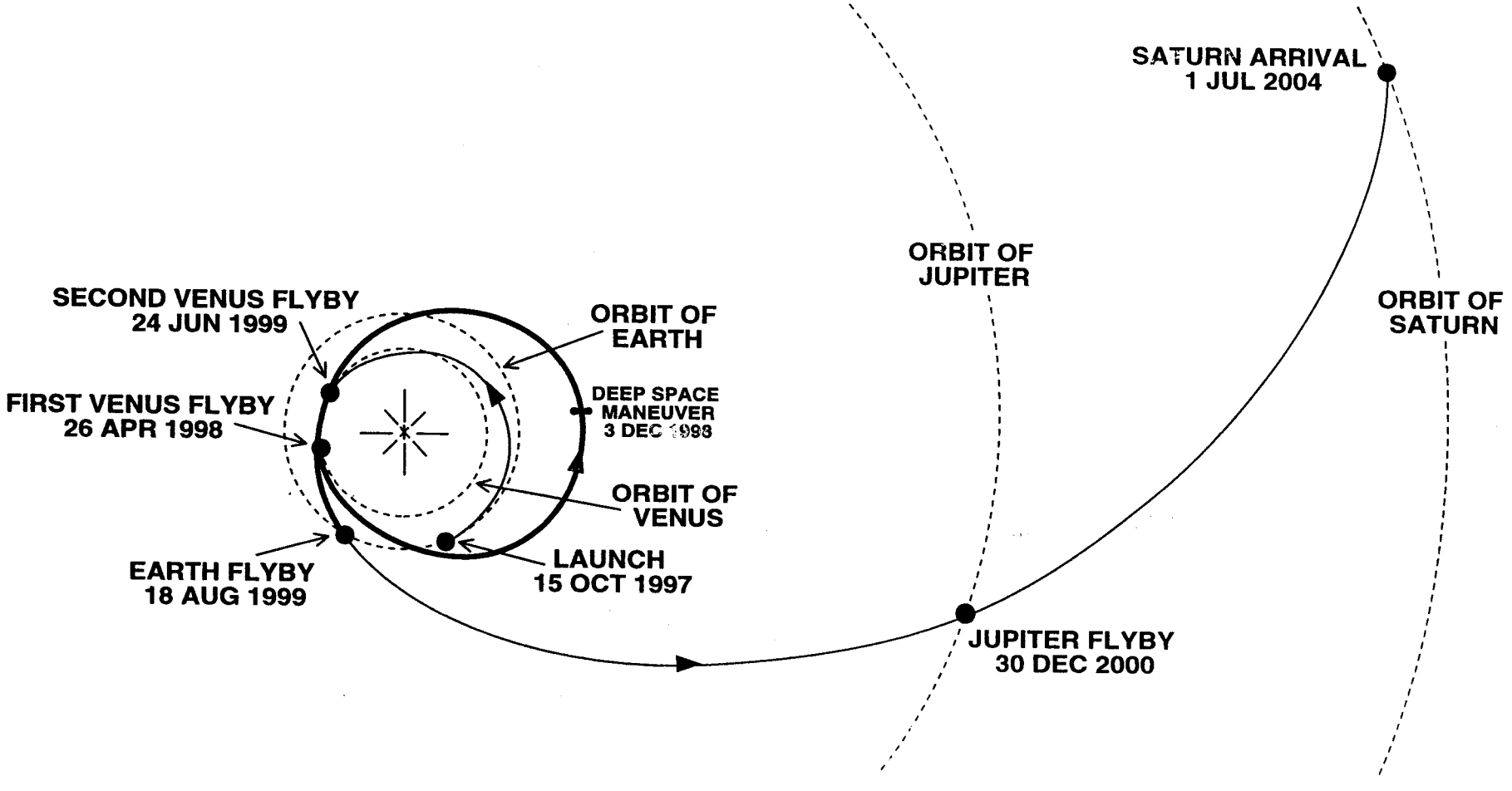
SATURN ARRIVAL
1 JUL 2004
ORBIT OF
JUPITER
ORBIT OF
SATURN
SECOND VENUS FLYBY
24 JUN 1999
ORBIT OF
EARTH
FIRST VENUS FLYBY
26 APR 1998
DEEP SPACE
MANEUVER
3 DEC 1998
ORBIT OF
VENUS
EARTH FLYBY
18 AUG 1999
LAUNCH
15 OCT 1997
JUPITER FLYBY
30 DEC 2000

Fig 2

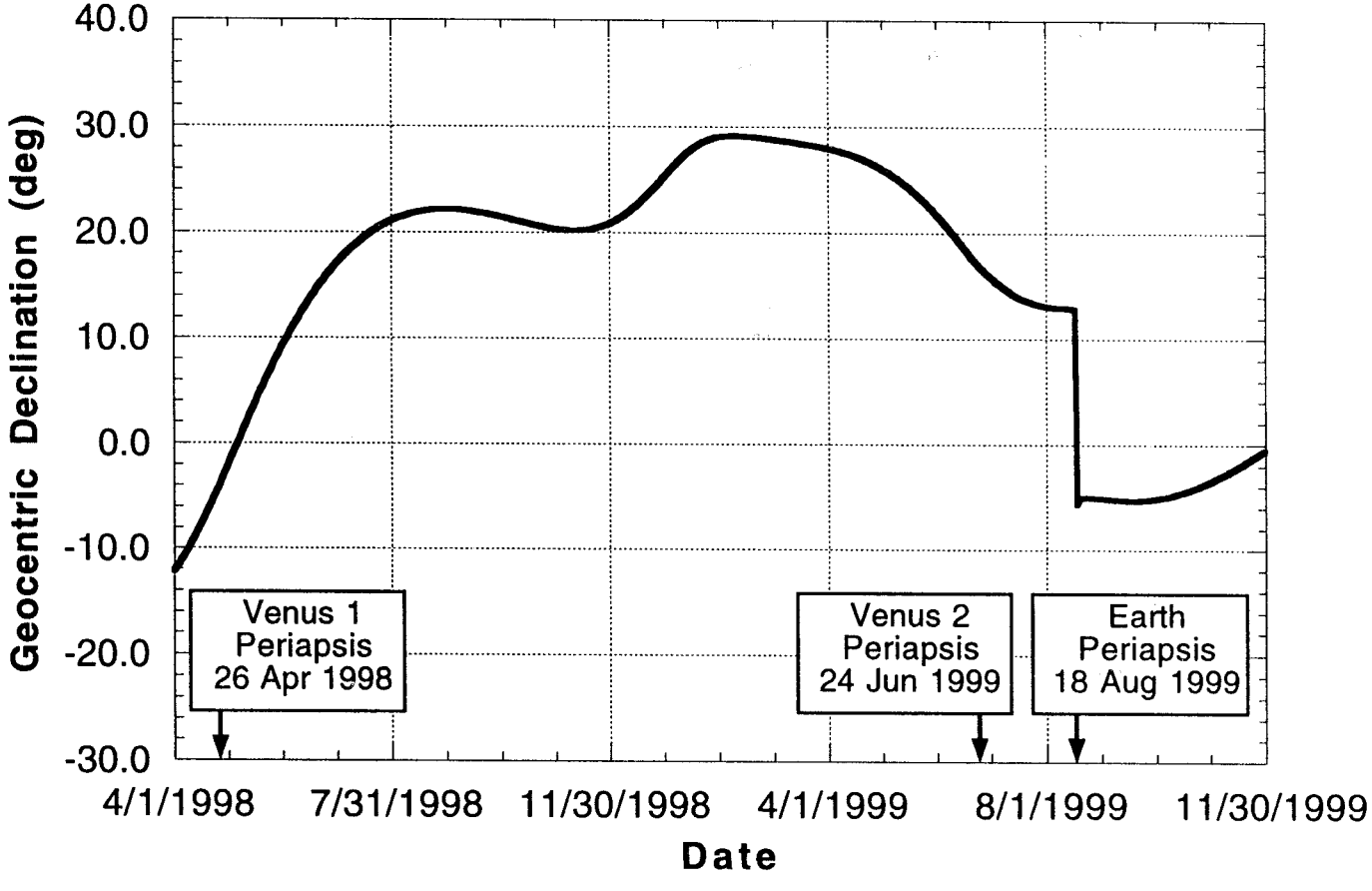
40.0
30.0
20.0
10.0
0.0
-10.0
-20.0
-30.0
Geocentric Declination (deg)
Venus 1
Periapsis
26 Apr 1998
Venus 2
Periapsis
24 Jun 1999
Earth
Periapsis
18 Aug 1999
4/1/1998
7/31/1998
11/30/1998
4/1/1999
8/1/1999
11/30/1999
Date

Fig 3

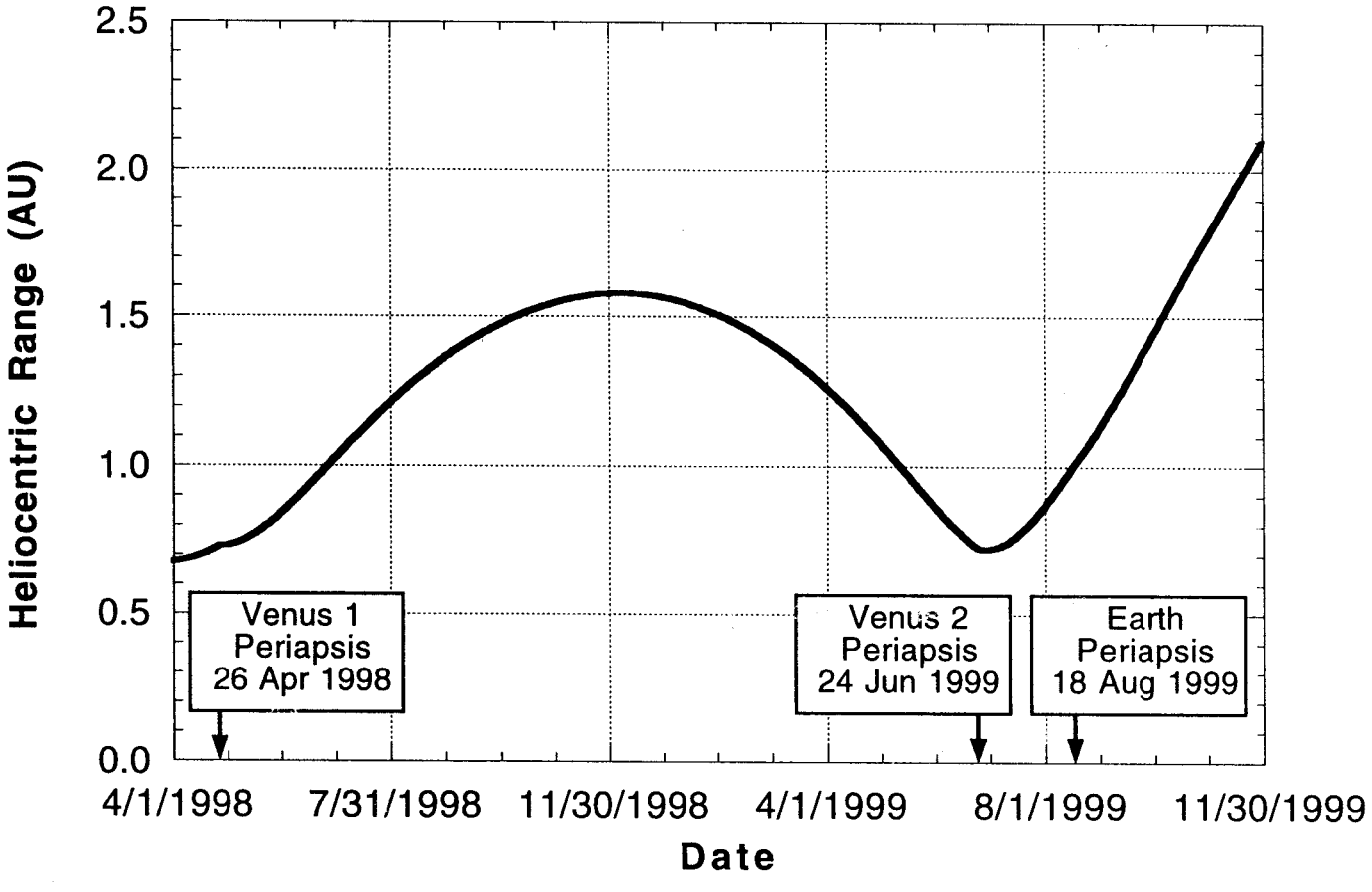
Heliocentric Range (AU)
2.5
2.0
1.5
1.0
0.5
0.0
Venus 1
Periapsis
26 Apr 1998
Venus 2
Periapsis
24 Jun 1999
Earth
Periapsis
18 Aug 1999
4/1/1998
7/31/1998
11/30/1998
4/1/1999
8/1/1999
11/30/1999
Date

Fig 4

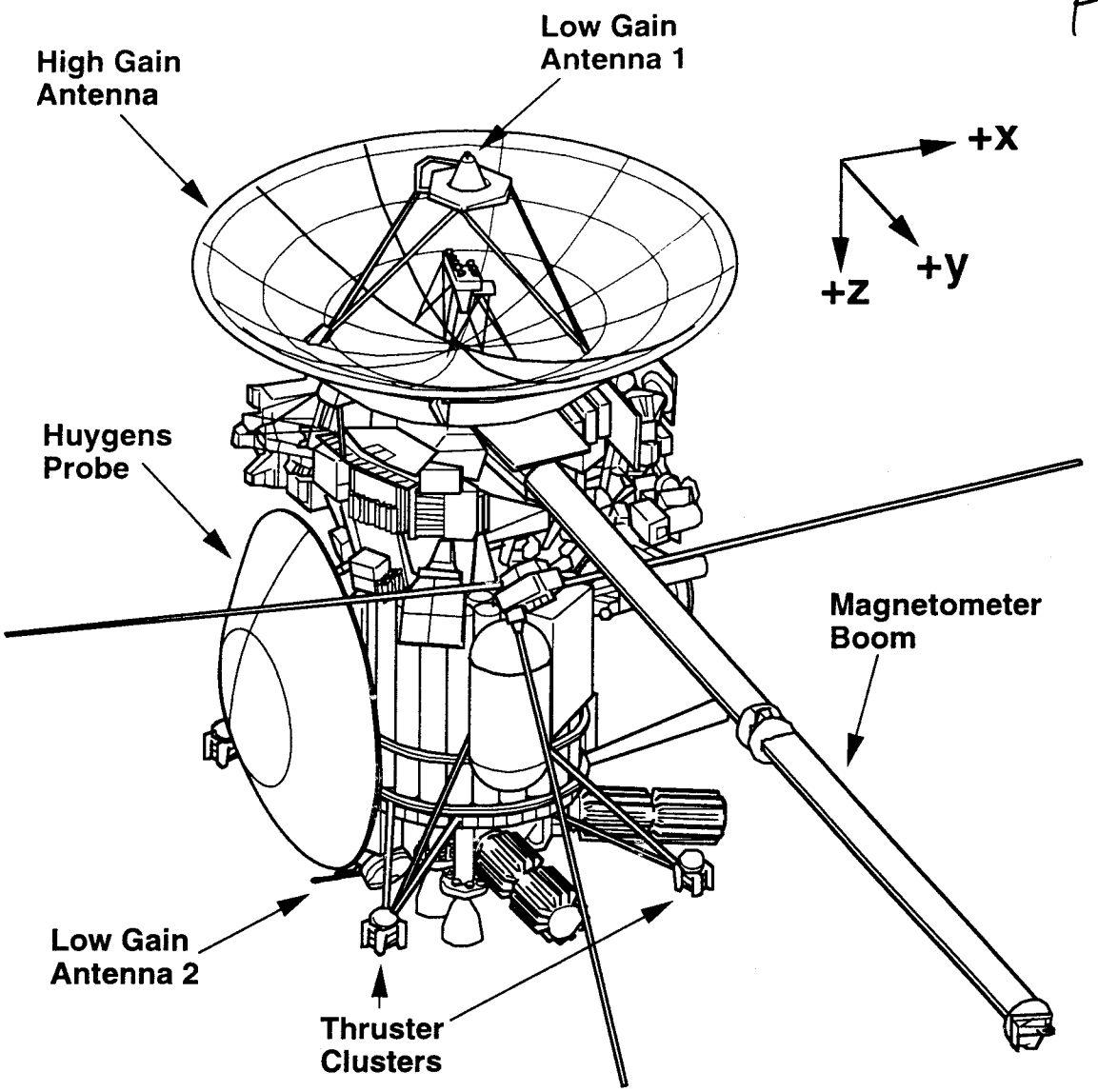
High Gain Antenna
Low Gain Antenna 1
+x
+y
+z
Huygens Probe
Magnetometer Boom
Low Gain Antenna 2
Thruster Clusters

Fig 5

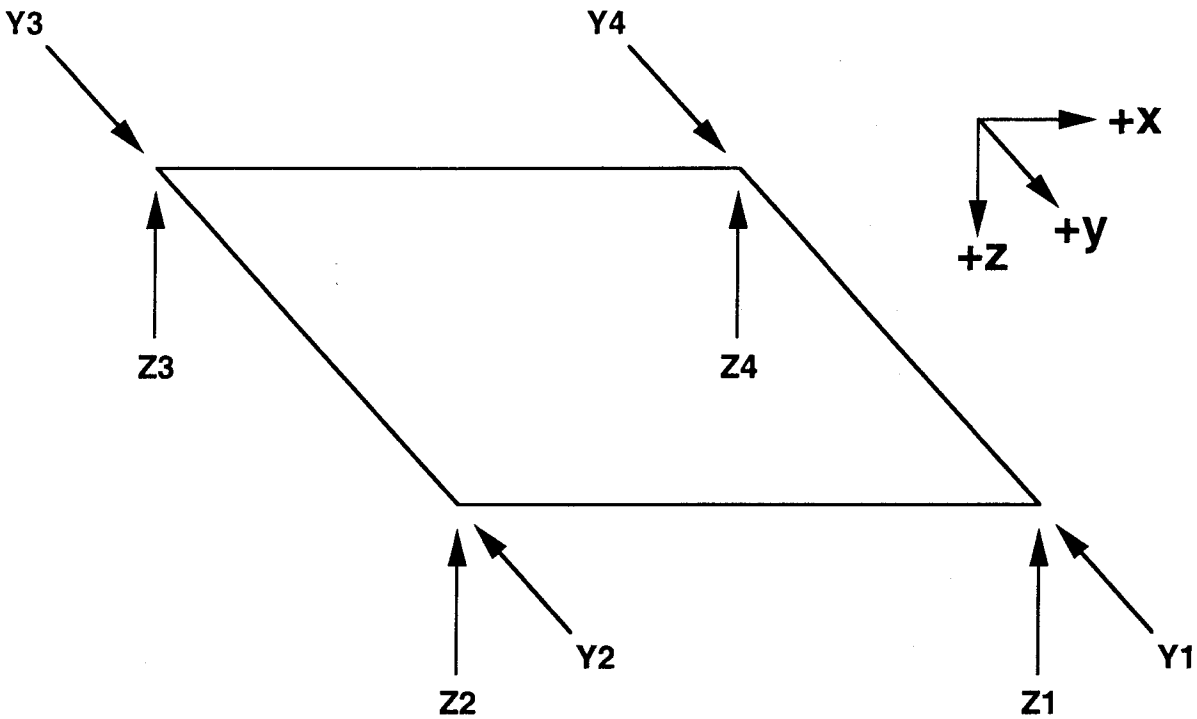

Fig 6

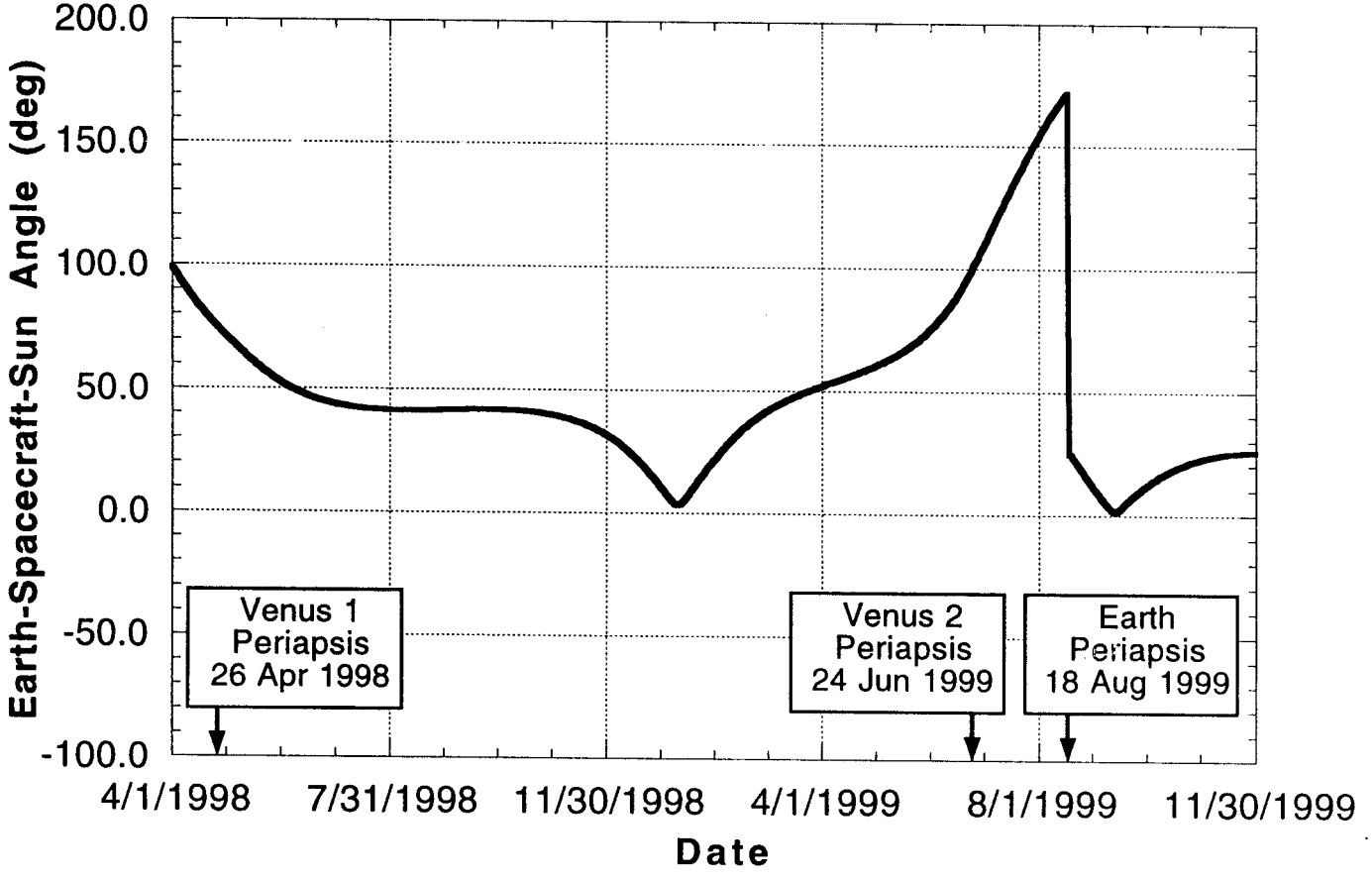
200.0
150.0
100.0
50.0
0.0
-50.0
-100.0
Earth-Spacecraft-Sun Angle (deg)
Venus 1
Periapsis
26 Apr 1998
Venus 2
Periapsis
24 Jun 1999
Earth
Periapsis
18 Aug 1999
4/1/1998
7/31/1998
11/30/1998
4/1/1999
8/1/1999
11/30/1999
Date

Fig 7

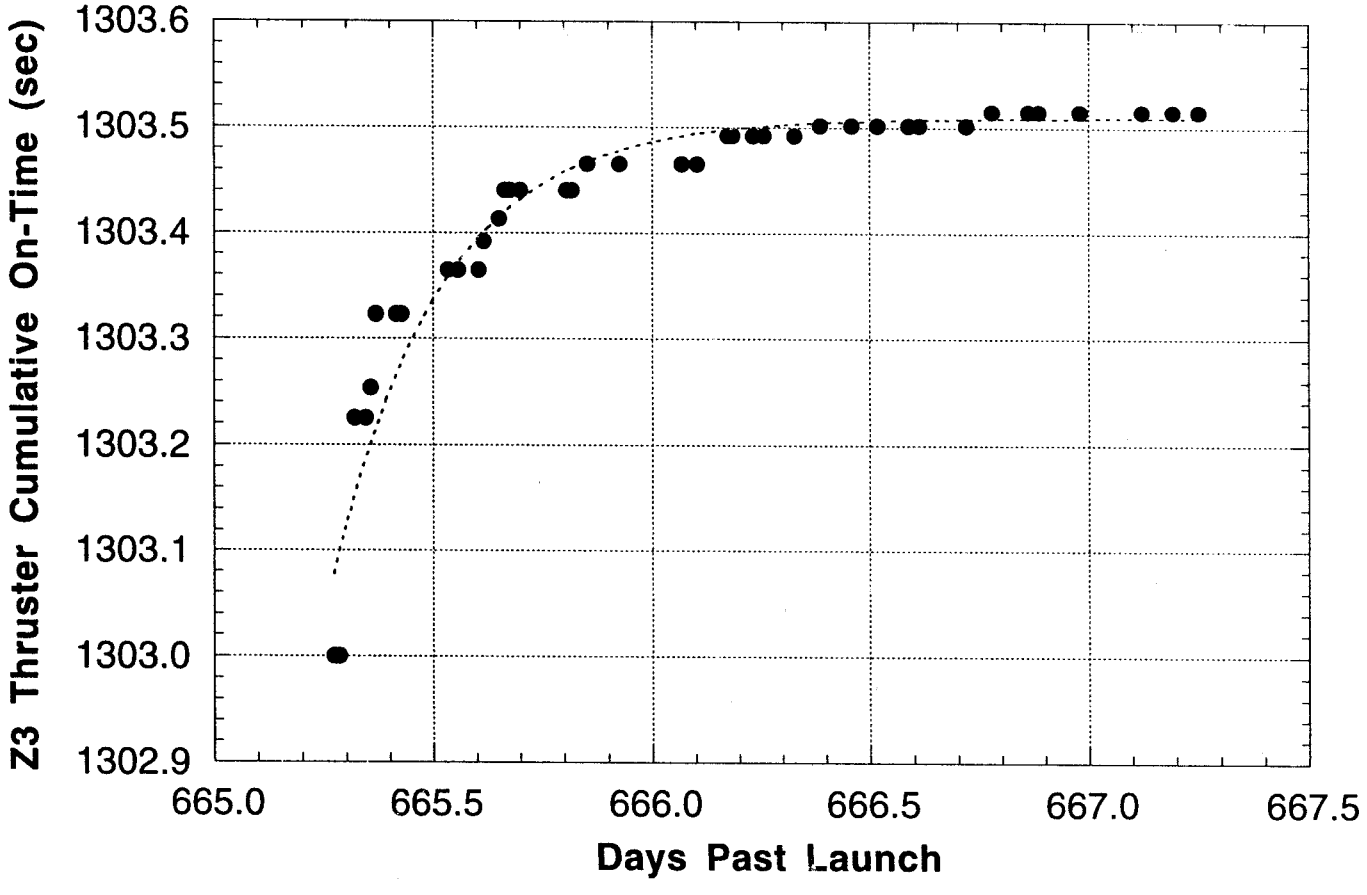
Z3 Thruster Cumulative On-Time (sec)
1303.6
1303.5
1303.4
1303.3
1303.2
1303.1
1303.0
1302.9
665.0
665.5
666.0
666.5
667.0
667.5
Days Past Launch

Fig 8

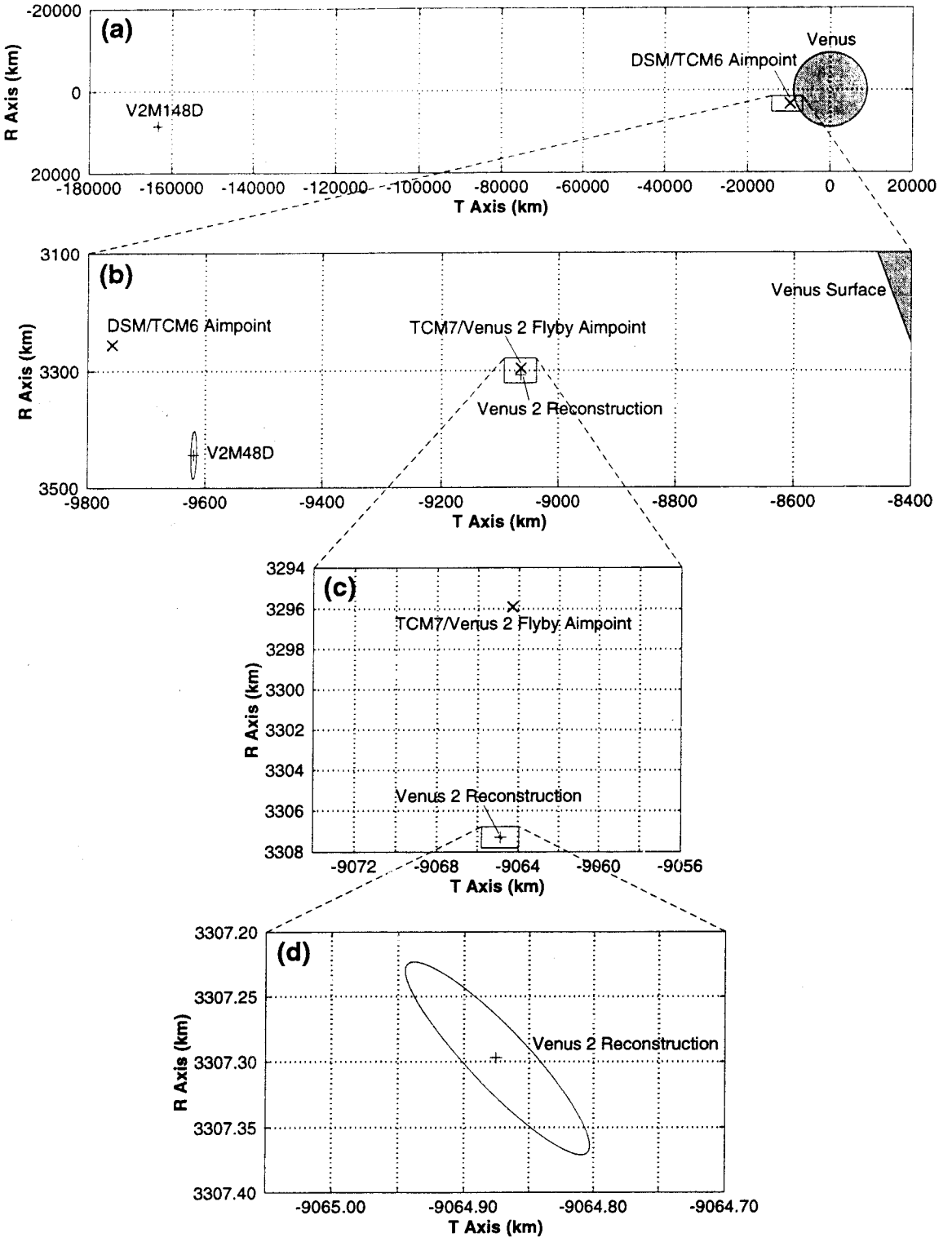
(a)
Venus
DSM/TCM6 Aimpoint
V2M148D
R Axis (km)
T Axis (km)
-20000
0
20000
-180000
-160000
-140000
-120000
-100000
-80000
-60000
-40000
-20000
0
20000
(b)
Venus Surface
DSM/TCM6 Aimpoint
TCM7/Venus 2 Flyby Aimpoint
Venus 2 Reconstruction
V2M48D
3100
3300
3500
-9800
-9600
-9400
-9200
-9000
-8800
-8600
-8400
(c)
TCM7/Venus 2 Flyby Aimpoint
Venus 2 Reconstruction
3294
3296
3298
3300
3302
3304
3306
3308
-9072
-9068
-9064
-9060
-9056
(d)
Venus 2 Reconstruction
3307.20
3307.25
3307.30
3307.35
3307.40
-9065.00
-9064.90
-9064.80
-9064.70

Fig 9

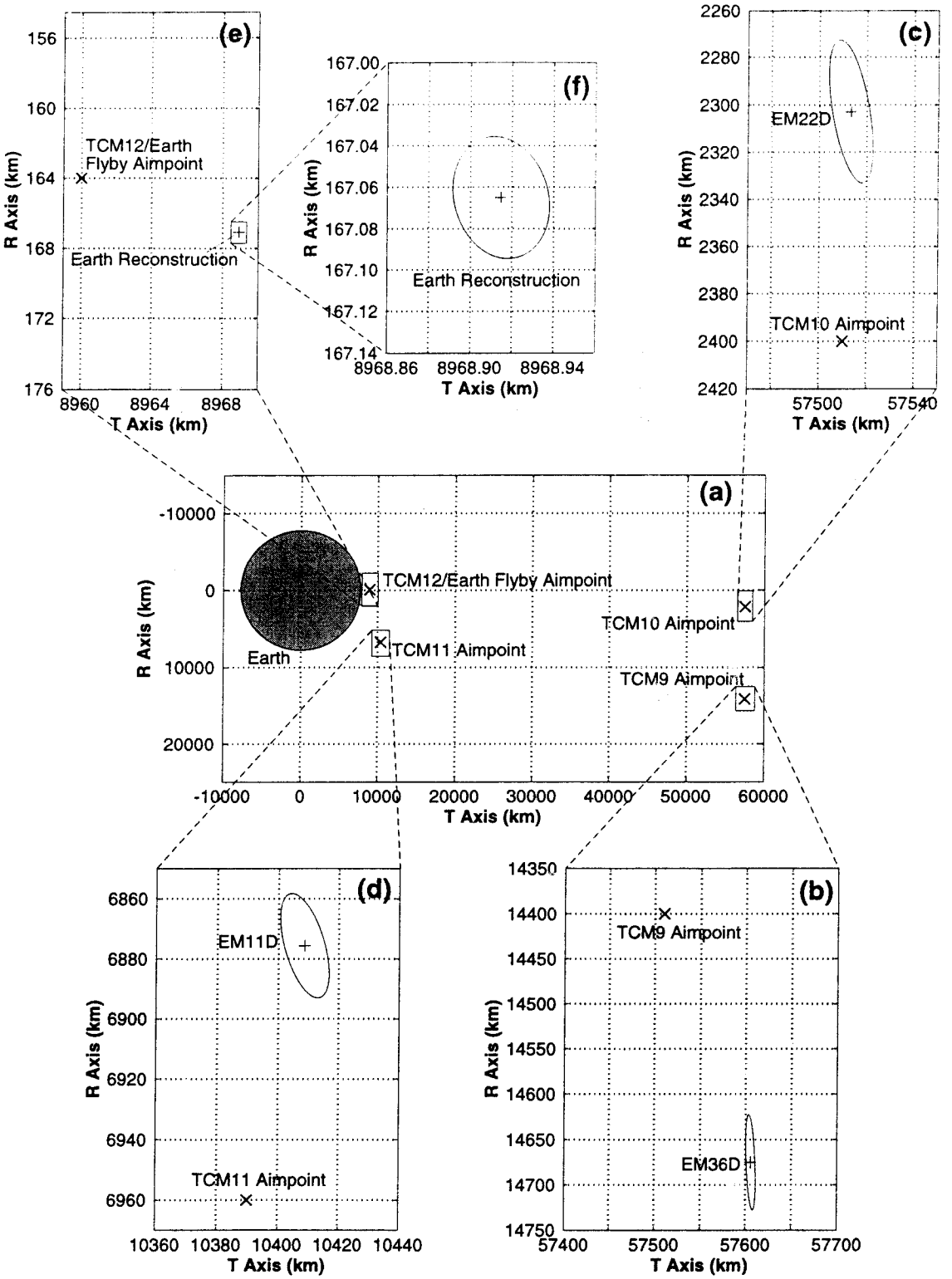
(a)
TCM12/Earth Flyby Aimpoint
TCM10 Aimpoint
TCM11 Aimpoint
TCM9 Aimpoint
Earth
R Axis (km)
T Axis (km)
(b)
TCM9 Aimpoint
EM36D
(c)
EM22D
TCM10 Aimpoint
(d)
EM11D
TCM11 Aimpoint
(e)
TCM12/Earth Flyby Aimpoint
Earth Reconstruction
(f)
Earth Reconstruction

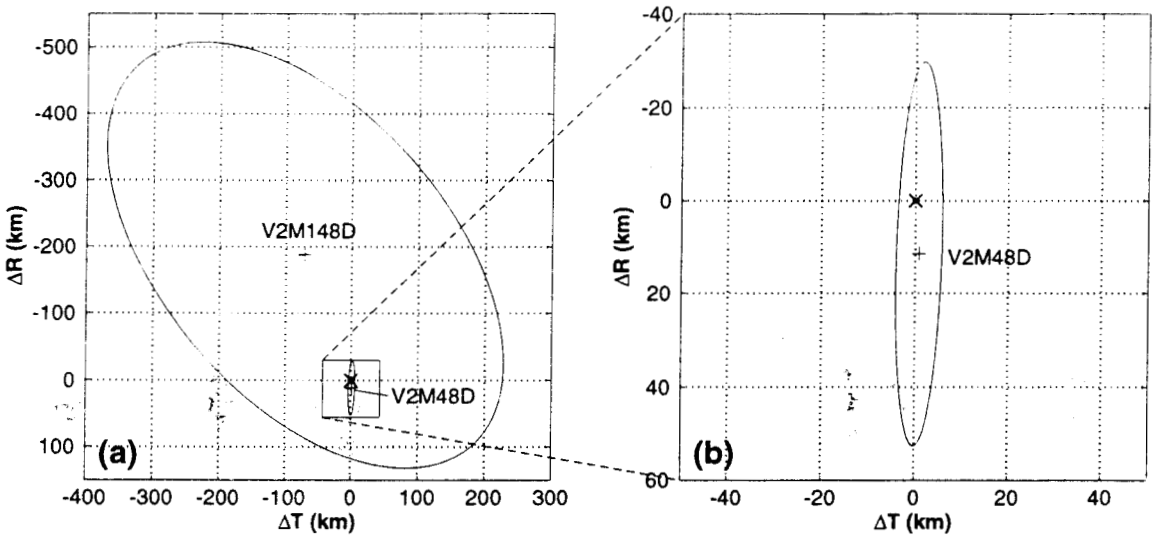
V2M148D
V2M48D
(a)
(b)
ΔR (km)
ΔT (km)

Fig 10

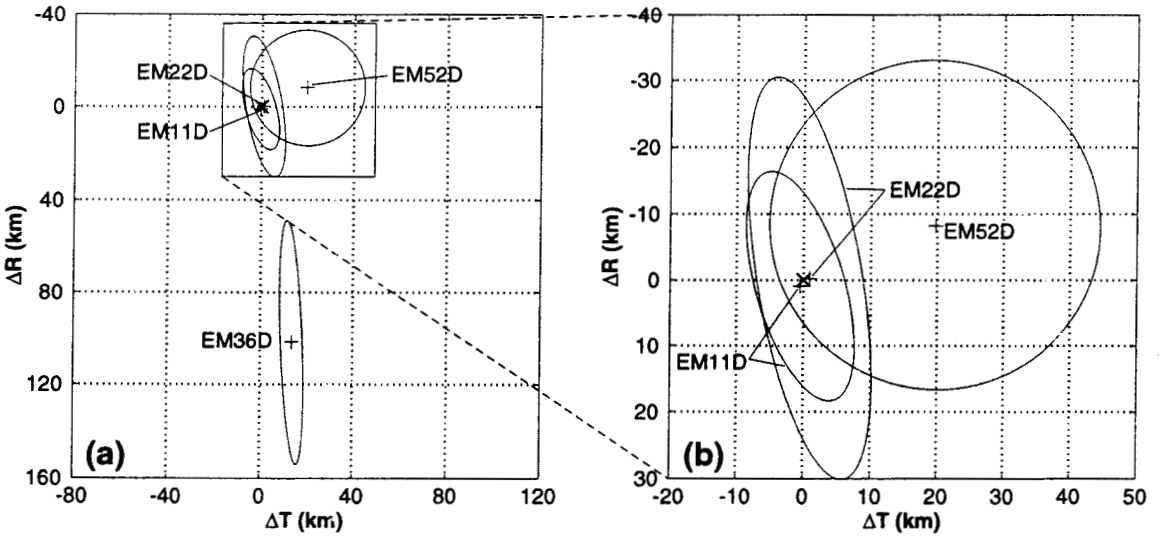
EM22D
EM52D
EM11D
EM36D
(a)
(b)
ΔR (km)
ΔT (km)

Fig 11

Figure 12a

V1 V2 F2

$\sigma = 0.03$ mm/s

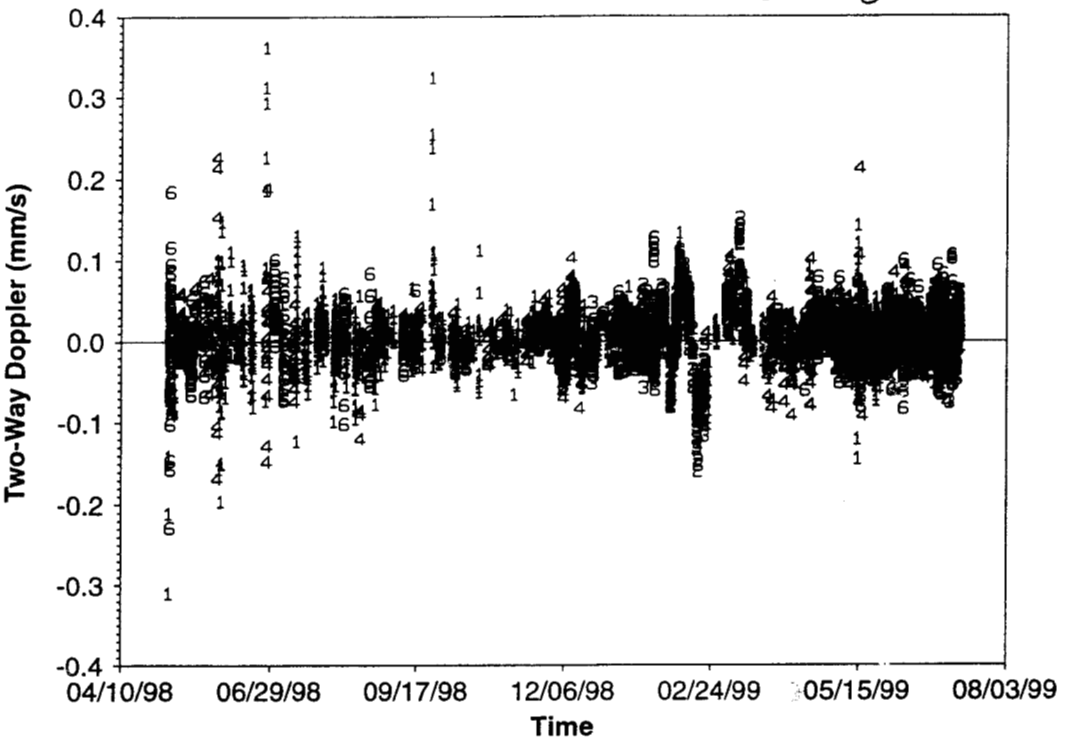

Figure 12b

V1V2 SRA
$\sigma = 5.27m$

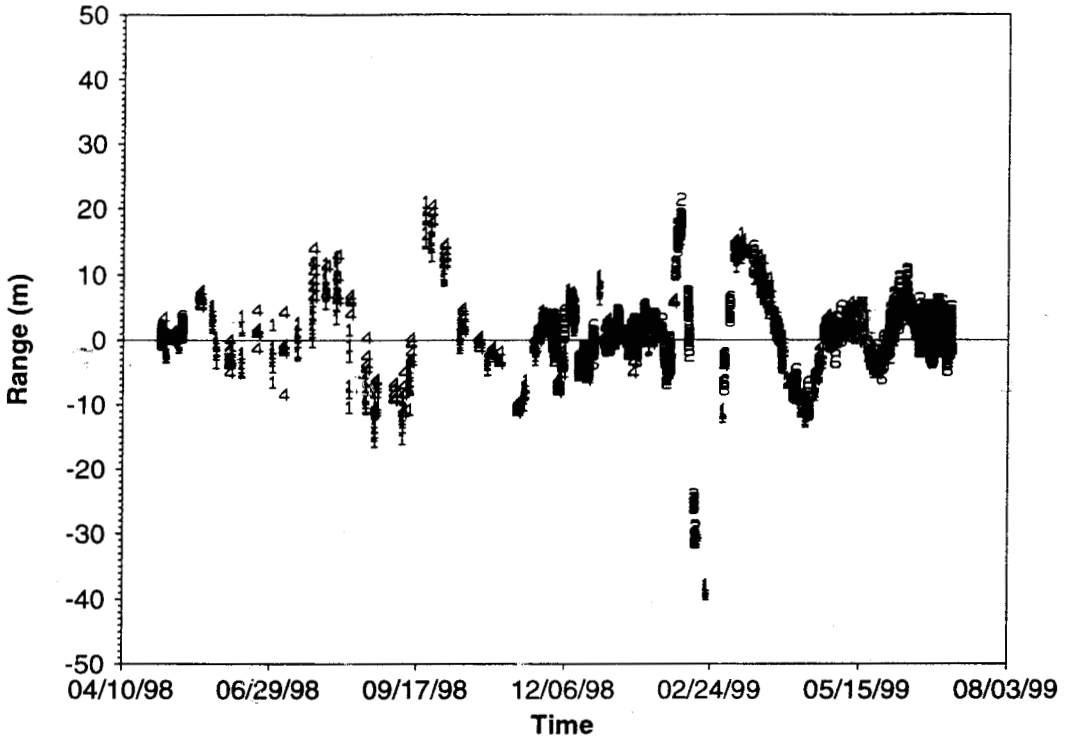

Figure 13a

V2E F2

σ = 0.02 mm/s

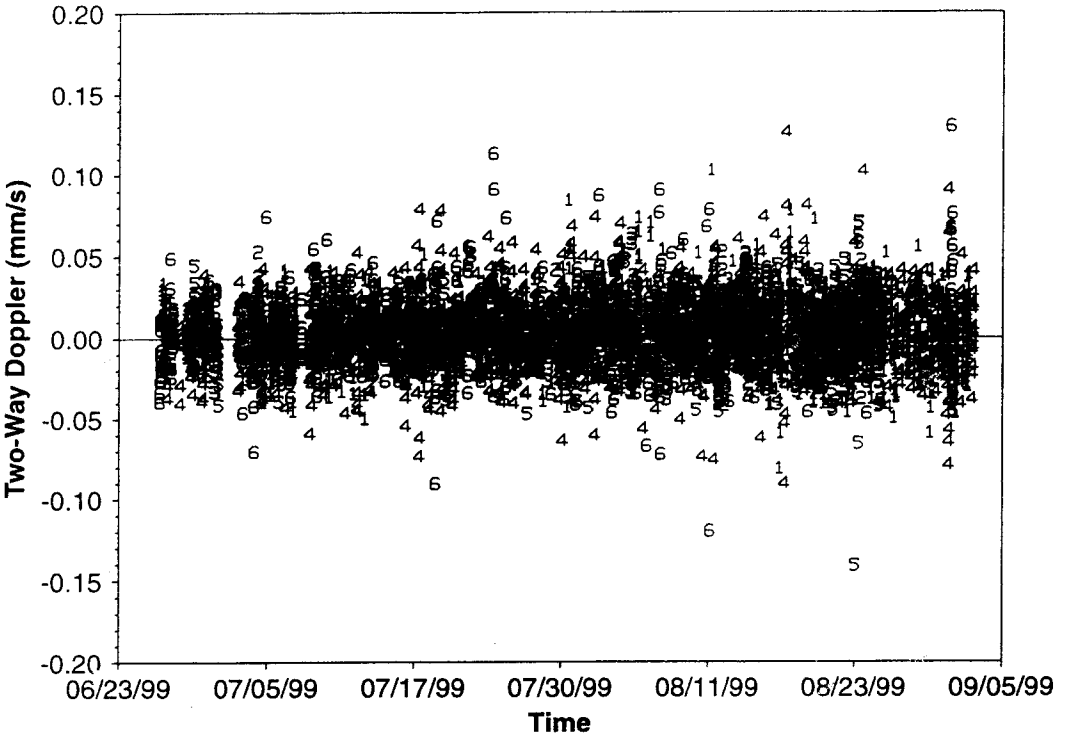

Figure 13b

V2E SRA

$\sigma = 0.75$ m

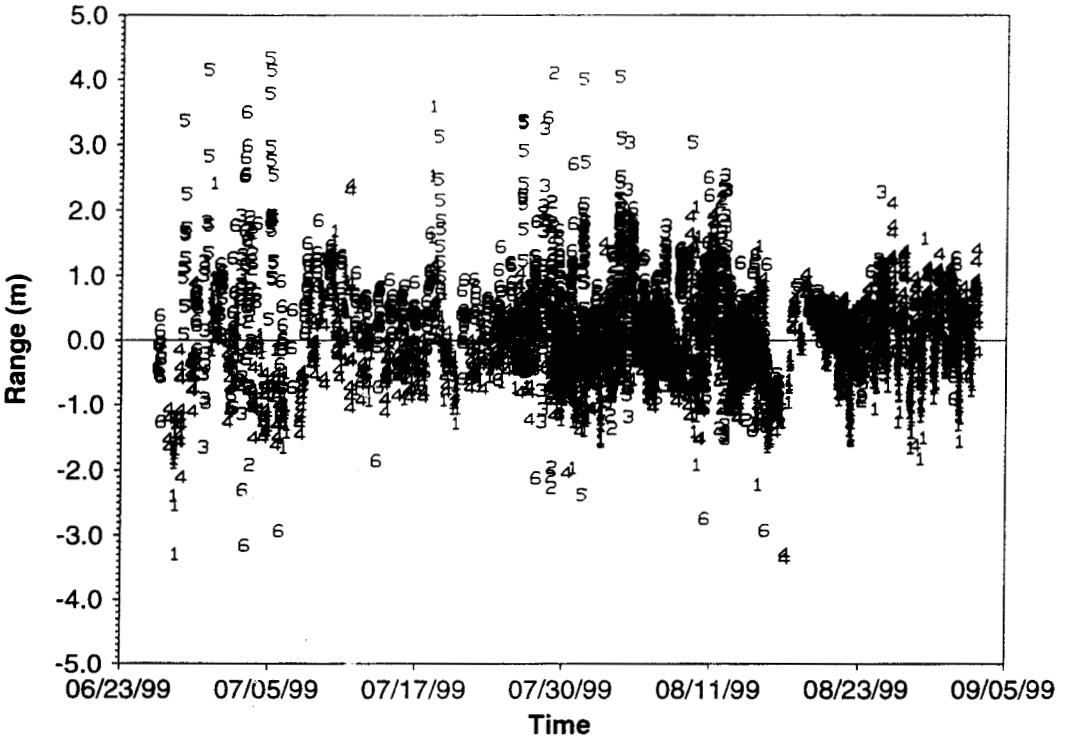

Fig 14

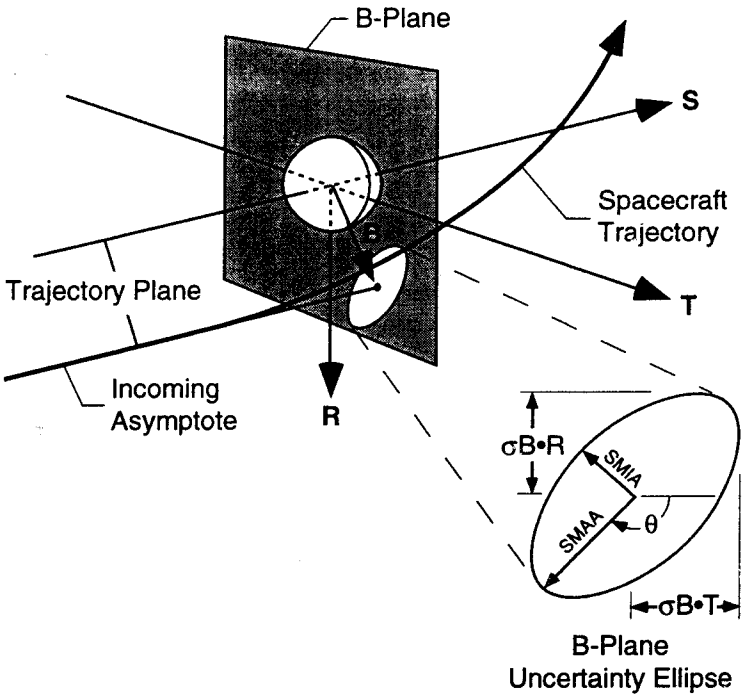
B-Plane
S
Spacecraft
Trajectory
Trajectory Plane
T
Incoming
Asymptote
R
σB•R
SMIA
SMAA
θ
σB•T
B-Plane
Uncertainty Ellipse